RESEARCH ARTICLE

Multiple Mobile Charger Charging Strategy Based on Dual Partitioning Model for Wireless Rechargeable Sensor Networks

YANG JIA, WANG JIAHAO, JI ZEYU, AND PENG RUIZHAO
College of Electrical and Electronic Engineering, Chongqing University of Technology, Chongqing 400054, China
Corresponding author: Wang Jiahao (wangjiahao.mail@foxmail.com)

ABSTRACT This paper proposes an online MMCCS (Multi-MC Cooperative Charging Strategy) for multiple Mobile Chargers (MC), affording static partition and dynamic collaboration. The developed scheme aims to solve the problem of high energy hole rates in Wireless Rechargeable Sensor Networks (WRSNs) by suggesting an on-demand charging architecture that minimizes the network's energy hole rate. Specifically, our strategy first establishes a dual-partition wireless rechargeable sensor network model to divide the service partition of the multi-mobile charging equipment and the charging request threshold partition of the Sensor Node (SN). Then based on this model, dynamic and collaborative multi-MC online charging path planning is performed to minimize the WRSN energy hole rate. The simulated trials challenge the proposed method against the NJNP (Nearest-Job-Next with Preemption), HC (Hamiltonian Cycle), and TSCCS (The temporal-spatial combined charging strategy) strategies, highlighting that the developed scheme reduces the average charging service distance of an MC, reduces the average waiting time of SN, and minimizes the WRSN's energy hole rate. Based on the simulation conditions, the WRSN energy void rate is 5.62%.

INDEX TERMS Wireless rechargeable sensor networks, cooperative charging, path planning, energy voids.

I. INTRODUCTION

A Wireless Rechargeable Sensor Network (WRSN) comprises several rechargeable sensors deployed in a specific area for event detection. WRSN has been broadly used in many fields, such as Industry 4.0 [1], environmental monitoring [2], home intelligence [3], and the Internet of Things [4]. Although researchers have extensively studied energy conservation in sensor networks [5], [6], [7], [8], battery limitations are still a bottleneck affecting the long-term operation of WRSNs. Existing research on sensor node energy replenishment focuses on three areas: node replacement [9], [10] energy harvesting [11], [12], [13], and Wireless Energy Transfer (WET) [14], [15], [16]. Due to the high cost of node replacement and the unpredictability of energy

The associate editor coordinating the review of this manuscript and approving it for publication was Adamu Murtala Zungeru [ID] .

harvesting [17], WET has played a revolutionary role in solving the energy lack in WRSNs. The main idea of WET is to charge the batteries of sensor nodes employing MC moving within the WRSN region [18]. Therefore, avoiding energy voids in the WRSN sensor nodes is crucial, which is achieved by determining the optimal charging path for the MCs. MC charging path planning research can be broadly classified into [19] single-MC and multi-MC.

Considering single MC path planning research, He *et al.* [20] proposed the classic NJNP strategy, which performs path planning based on the distance factor of the requesting charging node. This method has a low MC charging efficiency rate and high WRSN energy hole rate due to limitations in its path planning strategy. Lin *et al.* [21], [22] suggested a spatio-temporal collaborative path planning architecture addressing the low charging efficiency of MC. This solution created a charging path for MCs by prioritizing

the charging nodes based on temporal and spatial factors. This scheme effectively improves the MC's energy utilization but fails to effectively solve the WRSN's high energy void rate problem. In [23], the authors developed the mobile energy replenishment scheme ESAOC (Energy Starvation Avoidance Online Charging Scheme) to avoid node energy holes by calculating the maximum tolerable delay for each charging requirement and neglecting node death. Since the scalability of a single-MC WRSN system is low, by increasing the WRSN scale, the charging capacity of a single MC can hardly meet the network's energy consumption demand. So in large-scale WRSN, multiple MCs are required to charge the sensor nodes collaboratively and guarantee WRSN's stable operation.

Considering multi-MC path planning studies, numerous studies exploit a systematic planning strategy to treat path planning as a Traveling Salesman Problem (TSP) problem [24], [25], [26]. At the same time, the Hamiltonian Cycle [24], [25] and Genetic Algorithm (GA) [26] are employed to plan the multi-MC charging path, respectively. The periodic path planning strategy has a high MC energy utilization but ignores the node's dynamics. Hence, [27] proposed a partitioning strategy to charge each partition as a unit. This strategy disguisedly reduces the network's complexity and shortens the MC's charging travel distance but fails to consider the node's variability within each partition. Ying *et al.* [28] proposed TSCCS, a charging scheduling strategy that relies on a K-mean algorithm for partitioning and collaborative planning of the MC charging paths based on space-time. TSCCS effectively shortens the MC charging service distance and reduces the SN waiting time for charging. Nevertheless, all the above studies heuristically set a single charging request threshold and ignore the node's variability and dynamics, resulting in poor fairness of the MC charging response and an increase in the number of nodes with energy voids in the network [29].

Based on the problems of current literature, this work has the following innovative contributions. (1) Establishing a WRSN dual partition network model, where an improved K-means algorithm divides the multi-MC service partition to shorten the MC charging service distance and the SN charging waiting time. Furthermore, we develop an SN concentric circular charging request threshold partition that sets multiple charging request thresholds for SNs, improving the MC charging efficiency and guaranteeing the fairness of charging response. (2) Cooperative allocation based on charging suitability and multi-MC charging path planning aiming to minimize the energy hole rate of the WRSN.

II. WRSN NETWORK MODEL AND PROBLEM STATEMENT
A. WRSN NETWORK MODEL
This paper establishes the WRSN network model illustrated in Fig. 1, where the model is represented as (L, A, D, E, RE, R), with L the side length of the square area monitored by WRSN, $A = \{A_1, A_2, \cdots, A_i\}$ is the set
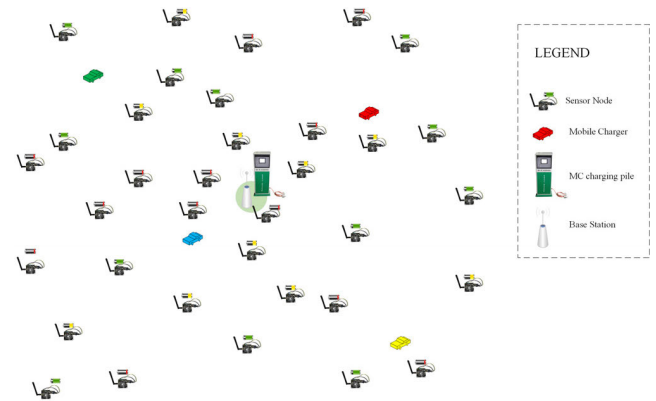

FIGURE 1. WRSN network model diagram.

of nodes in WRSN, and $D = \left(Eud\left(A_i, A_j\right) \middle| A_i, A_j \in A\right)$ denotes the set of Euclidean distances between the nodes, where $Eud\left(A_i, A_j\right)$ is the Euclidean distance between node A_i and node A_j. $RE = \left(RE_{A_i} \middle| A_i \in A\right)$ is the set of the node's remaining energy and $R = \left(R_{A_i} \middle| A_i \in A\right)$ denotes the set of the node's energy consumption. The WRSN system comprises three devices: Sensor Nodes, Base Stations (BS), and Mobile Chargers.

All SN in the network are equally equipped and are fixed after deployment, while the SNs have monitoring and communication capabilities. Specifically, the SNs send the area monitoring information and their energy announcements to the BS through multi-hop communication at intervals. Additionally, SNs send their charging request information to the base station as energy announcements when their remaining battery power is below the charging request threshold.

The node is equipped with a battery and a wireless energy receiver to receive the energy transmitted by the MC. At the center of the squared WRSN area, the BS has sufficient power and communication capability to receive and forward the charging requests from the SN and assign charging tasks to the MC through long-distance communication. The MC has autonomous mobility, computation, and communication capabilities, providing its energy through the BS. The device is equipped with a high-capacity battery and a wireless energy transfer device that uses electromagnetic effects or magnetic resonance coupling [31] to replenish the energy for the SN.

The energy notification model from the sensor node to the base station is $<ID_i, n, RE_{A_i}, ts_i, urg>$, where ID_i is the ID number of the sensor node, n is the energy notification sequence label, ts_i is the timestamp when sending data, and urg is the node's energy status. If $urg = 0$, the node has sufficient energy, i.e., the node's remaining energy is higher than the charging request threshold. If $urg = 1$, the remaining energy of the node battery is lower than the charging request threshold and the node requests energy replenishment. Only monitoring information is reported during the node's charging period, and no energy notice is sent. When charging completes, the energy notification sequence marker is set to one to notify the base station that charging has completed.

B. PROBLEM STATEMENT

1) MODEL ASSUMPTIONS

This paper makes the following assumptions for the WRSN network model.

Assumptions 1: The SN battery has limited capacity and needs MC to charge it for service. Suppose MC uses the OO (ONE to ONE) charging mode to charge the SN.

Assumptions 2: The energy consumption of SN to perform monitoring tasks is mainly data transmission consumption[22], and its energy consumption rate is assumed to be influenced only by the data transmission volume.

Assumptions 3: The MC has a limited battery capacity and needs to return to the base station for energy replenishment. It is assumed that the time for the MC to return to the base station for energy replenishment is only the elapsed time to move on the round-trip path[23], ignoring its battery charging time.

Assumptions 4: The energy consumption of MC is composed of three components: communication, mobile, and charging. Since the communication consumption is much lower than the mobile and charging consumptions[31], this paper assumes that the energy consumption of MC comprises mobile consumption and charging consumption.

Assumptions 5: The WRSN system adopts an unmanned operation and maintenance mode, and the MC has to retain enough energy to return to the BS for its energy replenishment after performing the charging service.

2) RELATED DEFINITIONS

In order to facilitate the discussion and analysis of the WRSN systems, we define the relevant concepts as follows.

Definition 1 (SN Energy Consumption Rate R_{A_i}): The remaining energy at the n-th energy notice of node A_i is $RE_{A_i(n)}$. The energy consumption rate at the n-th energy notice of node $R_{A_i(n)}$ is:

$$\begin{cases} R_{A_i(n)} = \dfrac{RE_{A_i(n-1)} - RE_{A_i(n)}}{\Delta}, & n \geq 2 \\ R_{A_i(1)} = \dfrac{E - RE_{A_i(1)}}{\Delta} \end{cases} \quad (1)$$

The energy consumption rate R_{A_i} of node A_i is always the calculated value at the time of the current energy announcement.

Definition 2 (SN Energy Hollow): The energy hole occurs when the battery of the SN is depleted and cannot maintain the normal operation. At time t, the remaining energy of the sensor node is:

$$RE_{A_i}(t) = RE_{A_i(n)} - (t - ts_i) R_{A_i} \quad (2)$$

If $RE_{A_i}(t) > 0$, the node $A(i,j)$ does not have an energy hole at the current timestep, and conversely, the node has an energy hole.

Definition 3 (WRSN Energy Void Rate): The WRSN energy hole rate is defined as the ratio of the number of energy-depleted nodes to the number of all nodes in the network.

When the number of energy hole nodes is large, it is prone to data loss.

Definition 4 (Network Lifetime): Energy voids in nodes in WRSNs can produce problems such as data loss, link failure and even network paralysis [29]. In this paper, by quantifying the state metrics of the WRSN, a network with an energy void rate of more than 15% is defined as paralyzed. Therefore, the network lifetime of a WRSN is defined as the operating time until the monitoring performance of the WRSN is not guaranteed[30].

Definition 5 (SN Maximum Survival Time $Delay_i(t)$): $Delay_i(t)$ is the time that the remaining energy of the current time sensor can maintain normal operation:

$$Delay_{A_j}(t) = \frac{RE_{A_j}}{R_{A_j}} + ts_j - t \quad (3)$$

If $Delay_{A_j}(t) \leq 0$, then the node is currently in the state of energy void.

Definition 6 (SN Average Charge Wait Time): We define the sensor node charging wait time as the interval from when a node sends a charging request to when the node is charged. The SN average charging wait time is the average charging wait time of all sensor nodes in the WRSN. If the charging waiting time of a node is too long, it indicates that the node cannot be charged in time after sending a charging request, which leads to the sensor node being prone to the energy hole situation.

Definition 7 (MC Average Charging Service Distance): The MC's average charging service distance is defined as the average distance an MC moves to charge the sensor node. The longer the average distance traveled, the more time and energy the MC spends on the path and the lower the energy utilization of the MC.

Definition 8 (Charging Suitability RCA): RCA is the degree of suitability of an MC for charging SN as an essential basis for MCs' collaborative decision-making. RCA is calculated as follows:

$$RCA = \frac{1 + \frac{RE_{MC}(t)}{P}}{1 + \frac{Eud(A_i, MC)}{max(Eud(A_i, A_j))}} \quad (4)$$

where $RE_{MC}(t)$ is the current remaining power of MC, P is the MC battery capacity, $Eud(A_i, MC)$ is the Euclidean distance between MC and SN, and $max(Eud(A_i, A_j))$ is the farthest Euclidean distance between two nodes in the sensor network.

III. DUAL PARTITION NETWORK MODEL

A. CHARGING SERVICE DIVISION

The network monitoring range is wide in large-scale wireless rechargeable sensor networks, involving many scattered nodes. In order to charge the nodes in the network in a more efficient and orderly manner, shorten the node charging waiting time, and reduce the number of energy-void nodes, this paper adopts a multi-MC cooperative charging strategy. The proposed solution uses an improved K-means algorithm

to cluster the entire network into K charging service partitions [27], thus reducing the MC charging service distance and the SN charging waiting time.

1) DETERMINING THE NUMBER OF MCS

The energy consumption of the WRSN system is mainly the energy consumption of the sensor nodes to carry out monitoring tasks. The node energy consumption is closely related to each node's dynamic energy consumption rate and the charging path of the MC, so it is difficult to accurately calculate the number of MCs required for the WRSN system.

For these reasons, this paper determines the number of MCs that guarantee the proper operation of the network by calculating the energy consumption and replenishment of the network as a whole [32]. Assuming that the MC charges a node at its maximum capacity, i.e., the MC charges a node without stopping to continue charging the next node, the average service time st of an MC to charge the node is the traveling time towards the node and the time to charge the node:

$$\begin{cases} st = \dfrac{(N+1)}{2}\left(\dfrac{d}{v} + \dfrac{E}{\eta}\right) \\ d = \dfrac{1}{N^2}\displaystyle\sum_{i=1}^{N}\sum_{j=1}^{N} Eud\left(A_i, A_j\right) \end{cases} \quad (5)$$

where N is the number of sensor nodes, E is the battery capacity of the sensor node, v is the movement speed of MC, η is the charging efficiency of MC, and d is the distance between any two nodes of the WRSN network. Based on the energy consumption and replenishment balance condition of the network, the total energy consumption rate of all nodes in the network should be less than the maximum charging efficiency of M charging carts:

$$\sum_{i=1}^{N} R_{A_i} \leq \frac{1}{st} ME \quad (6)$$

This paper utilizes a static partitioned charging strategy, i.e., the number of MCs equals the number of partitions. Thus, the minimum value of M is 3.764, and in order to improve the reliability and redundancy of WRSN, this work considers $M = K = 4$.

2) IMPROVED K-MEANS ALGORITHM FOR PARTITIONING MC SERVICES

The node locations $A = \{A_1, A_2, \cdots, A_i\}$ and the number of partitions K are known. The improved K-means algorithm divides N nodes into K sets S based on the physical distance between nodes and energy consumption rate similarity, such that the intra-group sum of squares is minimized [33] based on the objective function:

$$\underset{S}{arg\,min} \sum_{j=1}^{K} \sum_{A_i \in S_j} \left(R_{A_i} - R_{\mu_j}\right) \left\| A_i - \mu_j \right\|^2 \quad (7)$$

where μ_j is the mean value of all points in the cluster S_j and R_{μ_j} is the mean value of the energy consumption rate of all nodes in cluster S_j. This paper uses an iterative optimization approach for clustering [35] that initializes K randomly selected mean points $\left(m_1^{(1)}, \ldots, m_l^{(1)}, \ldots, m_K^{(1)}\right)$. This strategy considers the following two steps alternately.

Step 1. Distribution

Each node is assigned to clusters such that the sum of squares within the group is minimized such that the node is assigned to the nearest mean point with the highest similarity in energy consumption rate. Additionally, each node is assigned to only one defined cluster $S^{(t)}$, according to the distribution:

$$S_j^{(t)} = \left\{ A_i \left| \begin{array}{l} \left(R_{A_i} - R_{S_j}^{(t)}\right) \left\| A_i - m_j^{(t)} \right\|^2 \\ \leq \left(R_{A_i} - R_{S_l}^{(t)}\right) \left\| A_i - m_l^{(t)} \right\|^2 \\ \forall j,\, 1 \leq l \leq K \end{array} \right. \right\} \quad (8)$$

Step 2. Update

For each cluster obtained in the previous step, the center of mass of the observations in the cluster is used as the new distance mean point, and the average of the energy consumption rates of all nodes in the cluster is used as the new consumption rate mean point, i.e.:

$$\begin{cases} m_j^{(t+1)} = \dfrac{\displaystyle\sum_{A_i \in S_j^{(t)}} A_i}{\left| S_j^{(t)} \right|} \\[4mm] R_{S_j}^{(t+1)} = \dfrac{\displaystyle\sum_{A_i \in S_j^{(t)}} R_{A_i}}{\left| S_j^{(t)} \right|} \end{cases} \quad (9)$$

The improved K-means algorithm makes it more likely that nodes with similar physical distance and energy consumption rates will cluster into one class, reducing the variability of nodes. The algorithm converges when the allocation for the nodes no longer changes, and the clustering results are output. The improved K-means algorithm simulation yields the MC service partitioning model illustrated in Figure 2.

In this paper, the SN is divided into four clusters, i.e., the WRSN is divided into four service areas C_1, C_2, C_3, and C_4. Dividing an MC's charging service area can effectively reduce the system's computational complexity and the MC mobile energy consumption [34], which is more suitable for large-scale WRSN.

B. CHARGE REQUEST THRESHOLD PARTITION

If the SN charging request is set too large, i.e., the charging request is sent too early, the MC moves to the sensor node too early and charges the node, resulting in more charging requests per time from the network nodes, increasing further the energy consumption of the MC motion. If the SN charging request threshold is small, i.e., the charging request is sent too late, the maximum survival time of the sensor nodes is shortened, resulting in many nodes having energy holes
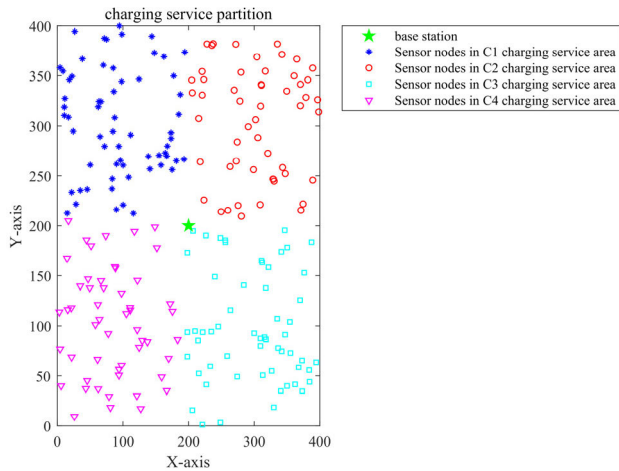
FIGURE 2. MC service division model.

FIGURE 3. Threshold partitioning model.

due to lack of timely charging. To address these problems, this paper divides the network into concentric circular zones and sets different charging request thresholds for the nodes in each circular zone based on the node survival rate to guarantee the fairness of the MC charging response.

1) THRESHOLD PARTITIONING MODEL

We divide the network into three layers of concentric circular threshold partitions $B_{n \in \{1,2,3\}}$. A higher charging request threshold is set for nodes further away from the base station, i.e., the sensor nodes at the edge have a longer maximum survival time to enable the MC to charge them in time. Accordingly, nodes close to the base station have a lower charging request threshold, i.e., the charging request of the nodes is delayed, improving MC energy utilization. The partitioning function of the distance clustering process is:

$$
\begin{cases}
B_1 = \left\{ A_i \middle| Eud\,(\mathrm{BS}, A_i) \leq \frac{1}{3} max\,(Eud\,(\mathrm{BS}, A_i)) \right\} \\
B_2 = \left\{ A_i \middle| \begin{array}{l} \frac{1}{3} max\,(Eud\,(\mathrm{BS}, A_i)) < Eud\,(\mathrm{BS}, A_i) \\ Eud\,(\mathrm{BS}, A_i) \leq \frac{2}{3} max\,(Eud\,(\mathrm{BS}, A_i)) \end{array} \right\} \\
B_3 = \left\{ A_i \middle| \frac{2}{3} max\,(Eud\,(\mathrm{BS}, A_i)) < Eud\,(\mathrm{BS}, A_i) \right\}
\end{cases}
$$

$$(10)$$

where $Eud\,(\mathrm{BS}, A_i)$ is the Euclidean distance between BS and node A_i. The simulation results of the threshold partition network model are depicted in Figure 3.

The concentric ring threshold of the sensor nodes within the WRSN is set to disperse the node's charging requests to shorten the MC's average charging service distance and reduce the SN's average waiting time.

2) CONCENTRIC CIRCLE CHARGE REQUEST THRESHOLD

(1) Charging request threshold with a single node survival rate as the target.

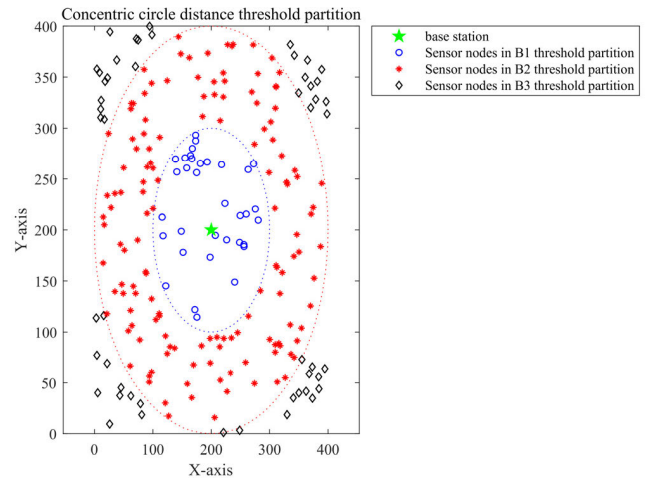Let node A_i send a charging request, and MC moves towards that node without stopping. The shortest

delay of the node is $t_{(\mathrm{BS}, A_i)}$:

$$
t_{(\mathrm{BS}, A_i)} = \frac{Eud\,(\mathrm{BS}, A_i)}{v} \qquad (11)
$$

Considering the single node survival rate as the target, the remaining energy of the SN should guarantee that the node operates appropriately within the minimum delay of waiting for charging.

Then the charging request threshold $E^1_{thred-B_n}$ of the threshold partition B_n should satisfy the energy consumption of all nodes in this partition, affording the shortest delay time of:

$$
E^1_{thred-B_n} > max\,\left(t_{(\mathrm{BS}, A_i)} \times R_{A_i}, A_i \in B_n \right) \qquad (12)
$$

(2) Charging request threshold with the network node survival rate being the target.

The charging waiting time of a node comprises two parts: the charging time of other nodes and the time of the MC path movement. Since the starting position of the MC charging service is located at the base station, the edge nodes have a longer waiting time for charging and a later charging response compared to the central node. Then the average charging waiting time wt_n of the nodes located within the concentric ring threshold partition B_n is:

$$
wt_n = \frac{\frac{d}{v} + \left(\frac{2d}{v} + \frac{E}{\eta} \right) + \cdots + \left(\frac{\left(\sum_{M=1}^{n} N_M \right) d}{Mv} + \frac{\left(\sum_{M=1}^{n} N_M - 1 \right) E}{M\eta} \right)}{\sum_{M=1}^{n} N_M}
$$

$$(13)$$

where N_M is the number of nodes in the charging service area C_M. Considering the network node survival rate as the target, the remaining power of the SN should be greater than the average energy consumption of the node during the charging service waiting period. Then the charging request threshold $E^2_{thred-B_n}$ of the threshold partition B_n should satisfy the

energy consumption of all nodes in the partition during the average charging waiting time:

$$wt_n = \frac{\frac{d}{v} + \left(\frac{2d}{v} + \frac{E}{\eta}\right) + \cdots + \left(\frac{\left(\sum\limits_{M=1}^{n} N_M\right)d}{Mv} + \frac{\left(\sum\limits_{M=1}^{n} N_M - 1\right)E}{M\eta}\right)}{\sum\limits_{M=1}^{n} N_M} \tag{14}$$

In summary, the charging request threshold $E_{\text{thred-}B_n}$ of the sensor nodes in the threshold partition B_n should satisfy the constraints of the single node survival rate and network node survival rate. The charging request threshold $E_{\text{thred-}B_n}$ for the thresholding partition B_n obtains the maximum value for $E_{thred-B_n}^1$ and $E_{thred-B_n}^1$, respectively, as shown in:

$$E_{\text{thred-}B_n} = max\left(E_{\text{thred-}B_n}^1, E_{\text{thred-}B_n}^2\right) \tag{15}$$

The simulation considers a concentric ring charging request threshold of $E_{\text{thred-}B_1} = 9.51\%E$, $E_{\text{thred-}B_2} = 14.33\%E$, and $E_{\text{thred-}B_3} = 16.21\%E$.

IV. MULTI-MC COLLABORATIVE CHARGING PATH PLANNING

A. PATH PLANNING ALGORITHM

This paper adopts the online charging strategy of static partitioning combined with a dynamic collaboration based on the dual-partition network model. Each charging service area is configured with a specific $MC_{M\in\{1,2,3,4\}}$ and separate charging service waiting areas $Z_{M\in\{1,2,3,4\}}$ are established, affording dynamic charging synergy between the MCs. The MMCCS strategy is based on the WRAN minimum energy void rate [36] to guide the multi-MC synergy for SN replenishment.

The basic idea of this strategy considers that if Z_M is non-empty, then MC_M determines whether the nodes that complete the charging service waiting for the area and do not have energy voids need to collaborate. When the nodes need to collaborate, BS divides them with the MCs based on the highest fitness and collaborative capability by comparing their charging fitness with other MCs. The MC_M after completing the cooperative division calculates the number of energy voids in the other nodes and the time to complete the charging task of the node when the node to be charged is the next charging node, respectively. This process always selects to charge the node that causes the least energy voids and completes the charging service moving the fastest to the next node to be charged under the precondition that the charging service can be returned to the base station. This strategy aims to minimize the number of energy voids in the network. The steps of the path planning algorithm for the MMCCS strategy are as follows.

Step1. Initialization. Establish the charging service waiting area Z_M, build the set Q of network death nodes, and establish a base station to assist in charging node collection Y.

Step2. Calculate the remaining power of each node to be charged in the charging service waiting area Z_M at the current time, remove the nodes with energy voids from the set Z_M and add them to the set Q.

Step3. Determine whether all charging tasks in the charging service waiting area Z_M must be coordinated when completed. The number of synergizing nodes CE_M of MC_M is:

$$\begin{cases} CE_M = \partial_M - a_M \\ \partial_M = \dfrac{RE_{MC}(t) - dc}{dc + E} \end{cases} \tag{16}$$

where ∂_M is the number of nodes where the MC_M's current remaining energy can complete the charging service and a_M is the number of nodes to be charged in the charging service area Z_M. If $CE_M > 0$, MC_M current remaining energy can complete the charging task, does not need synergy and has synergy capability. If $CE_M < 0$, MC_M needs synergy, and the $|CE|$ nodes with the smallest RCA value are added to set Y when the MC_M charging task is fully loaded and $CE_M = 0$.

Step4. The base station makes collaborative assignments to the nodes in set Y based on RCA. The nodes that need charging are sequentially assigned to the MC with the highest charging suitability and synergistic capability. The MC of the assigned collaborative node repeats **Step3** for collaborative capability judgment and completes the charging collaborative node division when the following equation is satisfied:

$$\begin{cases} (CE_M \geq 0, \forall M), & if\ (Y = \emptyset) \\ (CE_M = 0, \forall M), & if\ (Y \neq \emptyset) \end{cases} \tag{17}$$

Step5. Select the next charging node. MC_M always selects the node that causes the least number of energy voids in the node to be charged and requires the least time to complete charging as the next charging node. The charging priority A of the node to be charged is:

$$\begin{cases} F_i = COUNT\left(mwt_{(i,j)} > Delay_i(t), \forall j\right) + \dfrac{T_{ch}(i)}{\sum\limits_{i=1}^{a_M} T_{ch}(i)} \\ mwt_{(i,j)} = \dfrac{Eud(MC, A_i)}{v} + \dfrac{RE_{A_i}(t)}{\eta} + \dfrac{Eud(A_i, A_j)}{v} \\ T_{ch}(i) = \dfrac{Eud(MC, A_i)}{v} + \dfrac{E - RE_{A_i}(t)}{\eta} \end{cases} \tag{18}$$

where $mwt_{(i,j)}$ is the minimum charging waiting time of node A_j when node A_i is the next charging node, and the number of nodes with energy voids in Z_M at this time is $COUNT\left[mwt_{(i,j)} > Delay_i(t), \forall j\right]$. In this paper, the node with the smallest F_i-value is considered the next charging node.

Step6. Determine whether the remaining power of MC_M is sufficient to complete the charging task of the next node and then return to BS. The MC return energy

condition function is:

$$\begin{cases} E_{rest} = RE_{MC}(t) - E_{charge} - E_{back} \\ E_{charge(A_i)} = c \times Eud(MC, A_i) + (E - RE_i(t)) \\ E_{back} = c \times Eud(MC, BS) \end{cases} \quad (19)$$

where $E_{charge(A_i)}$ denotes the energy consumption of MC for charging services for node A_i. E_{back} indicates the energy consumption of the MC returning to the base station from the current position and $Eud(MC, BS)$ denotes the Euclidean distance of the node back to the base station. If $E_{rest} \geq 0$, then the next selected charging node is charged normally, and the node is removed from the charging service waiting area when charging is completed. If $E_{rest} < 0$, the MC returns directly to the base station to replenish its energy.

Step7. Determines whether the charging task is completed. If $Z_M \neq \varnothing$, return to **Step2**. If $(Z_M = \varnothing)$ and $(Q \neq \varnothing)$, select the node in the nearest set Q as the next charging node and return to **Step6**. If $(Z_M = \varnothing)$ and $(Q = \varnothing)$, MC_M returns to the base station to replenish energy and terminates the charging task.

The charging path planning code for MMCCS is shown in **Algorithm 1**.

B. STRATEGY EVALUATION

The MMCCS strategy minimizes the WRSN energy void rate by shortening the MC charging service distance and reducing the average SN charging wait time in five ways.

(1) The MMCCS strategy divides the charging service partition of multi-MC by the K-means algorithm, so that the MC can shorten the charging service distance and respond to the SN charging request more efficiently and quickly.

(2) The MMCCS strategy divides the SN charging request threshold partition and sets multi-level optimal charging request thresholds for sensor nodes, thus improving the fairness of charging responses.

(3) Whenever the next charging node is selected, MC always chooses the node that makes the smallest energy hole rate of WRSN.

(4) When multiple MCs collaborate, the base station assigns collaboration tasks based on the suitability of the SN and MC to ensure that the MC can efficiently and quickly replenish the SN.

(5) In the regression mechanism of MC, the nodes that already have energy holes are treated as nodes to be charged to reduce the number of nodes with energy holes.

The MMCCS flow chart is shown in Fig. 4.

V. SIMULATION AND ANALYSIS
A. SIMULATION PARAMETERS

Since WRSN is widely used in environmental monitoring and its network size ranges from 100m × 100m to 800m × 800m [2], we utilize MATLAB-2018a to simulate the sensor nodes randomly that spread in a square WRSN network with a side length of 400m. The simulated network bandwidth is 10Kbps, and the energy consumption per unit amount of

---

Algorithm 1 Pseudo-Code of Path Planning Algorithm for MMCCS Policy

Input: Set of nodes to be charged Z_M
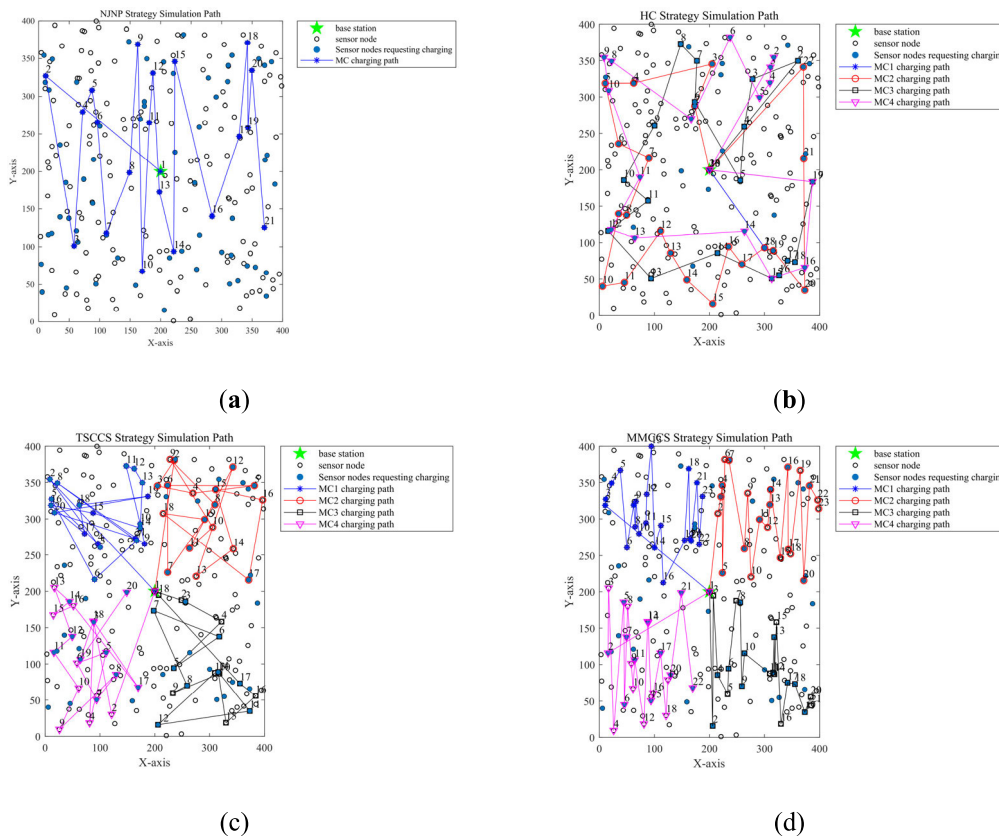**Output:** Next charging node A_m

```
1.    While Z_M ≠ Ø or Q ≠ Ø do
2.      {Initialization: A_m=null; Q=null; Y=null; M=4; K=0;
3.      For m = 1, m ≤ M, m++
4.       If Z_M ≠ Ø, then
5.        For i = 1, i ≤ size(Z_M), i++
6.         Calculate RE_{A_i}(t) according to equation (2);
7.         If RE_{A_i}(t) < 0, then
8.          Delete A_i in Z_M; K=K-1;
9.          Add A_i to Q;
10.         Else K=K+1;
11.        End if
12.       End for
13.       For i = 1, i ≤ K, i++
14.        Calculate RCA(i) according to equation (4);
15.        Calculate CE_M according to equation (16);
16.       End for
17.       If CE_M < 0, then
18.        For j = 1, j ≤ |CE_M|, j++
19.         Delete A_j with the minimum RCA(j);
20.         K=K-1;
21.         Add A_j to Y;
22.        End for
23.       Else
24.        For i = 1, i ≤ size(Y), i++
25.         Add A_i to Z_M with Maximum RCA(i);
26.         K=K+1;
27.         If CE_M = 0, then
28.          Break
29.         End if
30.       End if
31.       For i = 1, i ≤ K, i++
32.        Calculate F_i according to equation (18);
33.       End for
34.       A_m = A_i with the minimum F_i;
35.      Else
36.       If (Q ≠ Ø), then
37.        For i = 1, i ≤ size(Q), i++
38.         Calculate Eud(A_i, MC_M);
39.        End for
40.        A_m = A_i with the minimum Eud(A_i, MC_M);
41.       End if
42.      End if
43.      Calculate E_rest according to equation (19);
44.      If E_rest ≥ 0, then
45.       Charging for the next node;
46.      Else
47.       MC_M return to the base station;
48.      End if
49.     End for
```

data received and sent by the sensor nodes is 1mJ and 3mJ, respectively [23]. The generation of monitoring data obeys

FIGURE 4. The MMCCS flow chart.

TABLE 1. Simulation default parameters table.

Simulation parameters	Value
Number of sensor nodes (N)	200
SN's battery capacity (E)	100（J）
SN message transmission time interval (Δ)	30（s）
Battery capacity of MC (P)	5000（J）
MC's movement speed (v)	5（m/s）
Charging efficiency of MC (h)	300（mJ/s）
MC Mobile Energy Consumption (c)	30（mJ）

a Poisson distribution with a mean interval of 60s and a simulation duration of 60000s. Table 1 reports the default simulation parameters.

To evaluate the performance of MMCCS, the performance metrics used in this paper are the average SN waiting time, the average MC charging service distance, the WRSN energy void rate, and the network lifetime.

B. CROSS-SECTIONAL ANALYSIS
The proposed strategy is challenged against NJNP [20], HC [24], and TSCCS [28]. The evaluation is cross-sectional to analyze and evaluate the MMCCS strategy's performance comprehensively. In the simulation experiments, only the NJNP strategy uses a single MC for charging service, while

TABLE 2. Comparison of strategy simulation results.

Strategies	SN average waiting time（S）	MC average charging service distance（m）	WRSN energy void rate（%）
NJNP	382.3	261.2	31.25
HC	221.6	173.0	11.08
TSCCS	197.2	134.5	7.71
MMCCS	172.3	121.7	5.62

the remaining strategies are multi-MC, and the number of MCs is four.

Table 2 reports the simulation results of the four strategies, highlighting that the MMCCS strategy has a shorter average MC charging service distance, a reduced average SN waiting time, and a smaller WRSN energy hole rate. Compared with the TSCCS strategy, the proposed strategy can reduce the WRSN energy hole rate by 27.11%.

The MC single cycle path planning is illustrated in Figure 5. The NJNP strategy in Fig. 5a provides path planning based on the proximity principle and uses a single MC for charging service. Thus, the number of nodes completing charging in a single cycle is much lower than the number of requested charging nodes in WRSN. Additionally, the average MC charging service distance is significantly lower than the other three strategies. The HC strategy in Fig. 5b uses periodic path planning with MC charging paths for Hamiltonian circuits. Compared with the NJNP strategy in Figure 5a, the HC scheme adopts a multi-MC charging service strategy that significantly improves the system's charging service capacity and shortens the charging distance of MC. Nevertheless, the HC strategy does not divide the multi-MC service area, and its number of charging service nodes in a single cycle is lower than that of TSCCS and MMCCS. The TSCCS strategy in Fig. 5c carries out online path planning based on spatio-temporal cooperation utilizing a multi-MC charging service strategy. Compared with NJNP and HC, it can effectively reduce the MC charging service distance and the waiting time of SN charging. The MMCCS strategy in Fig. 5d adopts a static partitioning plus dynamic cooperative strategy compared with the previous three strategies, and sets a concentric circular charging request threshold for the nodes, which makes the MC charging response fairer, the path planning efficient and reasonable, increases the number of MC service nodes in a single cycle, and shortens the MC charging service distance.

C. LONGITUDINAL ANALYSIS
This paper focuses on a longitudinal multi-level comparative analysis by discussing the impact of four aspects on strategy performance: the number of nodes, the MC capacity, and the charging efficiency of MC to SN, the number of MC.

1) IMPACT OF THE NUMBER OF NODES ON PERFORMANCE
The following experiments discuss the interplay between the number of nodes and each strategy's performance.

FIGURE 5. Example diagram of the single-cycle operation of the four strategies. (a) NJNP Strategies; (b) HC Strategies; (c) TSCCS Strategies; (d) MMCCS Strategies.

We consider that the number of sensor nodes gradually increases from 40 to 400 with a 40-node interval, while the other parameters are preserved to their default values. The performance of each strategy is illustrated in Fig. 6, revealing that when the number of nodes is 160-280, the network charging response is more equitable, and the number of nodes with energy voids is reduced. The comparison results show that the MMCCS strategy has excellent applicability and can be extended to networks with a larger number of sensor nodes.

Fig. 6a indicates that the average SN waiting time for all four strategies has an increasing trend as the number of nodes increases. This is because, as the number of nodes increases, more nodes must be charged in the WRSN, and the time delay of the MC movement towards the nodes increases. Therefore, the nodes wait longer for charging. The NJNP strategy considers single MC charging, while the other three strategies exploit multi-MC charging, resulting in the charging capability of the NJNP strategy being much lower than the other strategies and the average node waiting time being significantly higher.

In Fig. 6b, the average MC charging service distance of all four strategies decreases as the node cardinality increases. Given that the range of WRSN is fixed and the density of the sensor nodes increases when the number of nodes increases, the distance between the nodes decreases, and the average MC's charging service distance decreases. Changing

the sensor node density in the NJNP strategy has a limited impact on the average MC charging service distance compared with the other three strategies, resulting in the slow decrease of its average MC charging service distance with the increase of nodes. The HC strategy does not divide the charging service area and uses the Hamiltonian loop algorithm to periodically plan the multi-MC charging path of the entire network, resulting in a slightly higher average MC charging service distance than the TSCCS and the MMCCS strategies.

Fig. 6c highlights that all four strategies' WRSN energy hole rate increases as the number of nodes increases. The number of nodes requesting charging in the network increases with the number of nodes. When the number of sensor nodes is small, the number of nodes requesting service does not exceed the service capacity of the MC, and the MC can replenish the energy of the nodes to be charged relatively quickly. Thus, all four strategies' WRSN energy hole rates are not significant. However, when the number of nodes in the WRSN network gradually increases to 120, the WRSN energy hole rate of the NJNP strategy shows a significant increase, and when the number of nodes gradually increases to 200, the energy hole rate of the other strategies increases significantly. The MMCCS strategy adopts an on-demand charging architecture and selects the next charging node based on the minimum WRSN energy hole rate. Hence, the
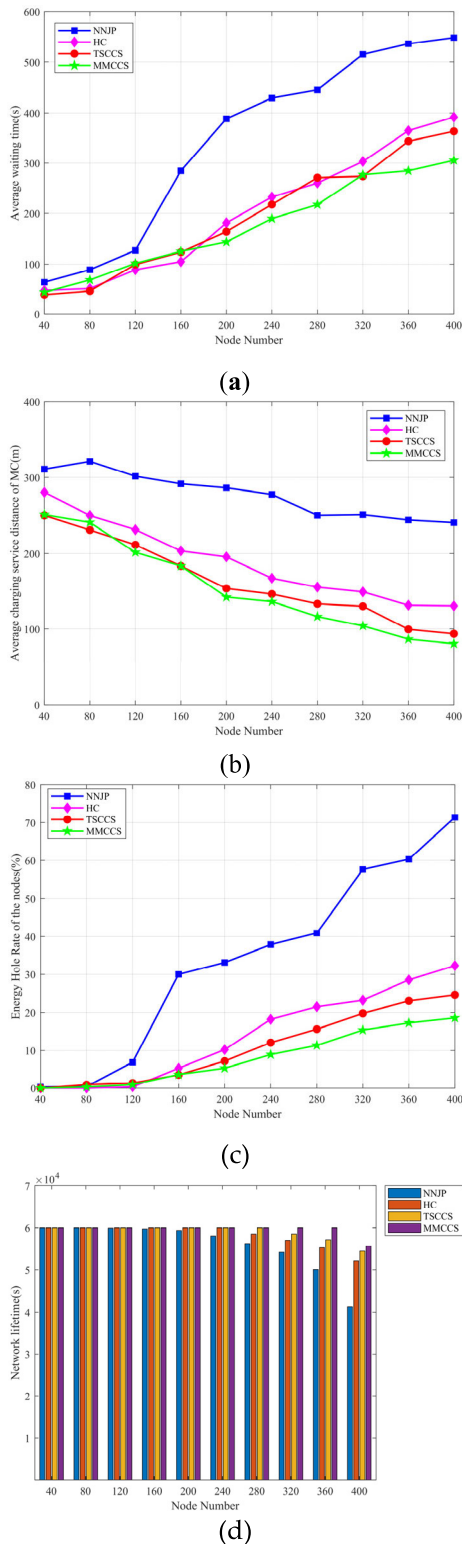
FIGURE 6. Impact of the number of nodes on network performance. (a) SN average waiting time; (b) MC average charging service distance; (c) WRSN energy void rate;(d) Network lifetime.

MMCCS strategy has a lower WRSN energy hole rate than the TSCCS strategy under the same number of MCs.

Fig. 6d shows that the MMCCS strategy has a more extended network lifetime for the same number of sensor

nodes. As the number of nodes increases, the sensor network has a greater energy demand. Since NJNP uses the charging mode of single MC, its network survival time first appears to be shortened and shows an accelerated decreasing trend. When the number of nodes increases to 280, the network survival time of the HC strategy and TSCCS strategy appear short successively, while the network lifetime of the MMCCS strategy only starts to decline when the number of nodes increases to 360.

2) IMPACT OF MC CAPACITY ON PERFORMANCE

The subsequent trials discuss the influence of MC capacity on the performance of each strategy. For this trial, the sensor node capacity gradually increases from 1000J to 10000J at an interval of 1000J, while the other parameters are the default. The corresponding performance change per strategy is depicted in Figure 7, highlighting that the proposed charging planning scheme is efficient and reasonable.

Fig. 7a reveals that the average SN waiting time of all competitor strategies gradually decreases as the MC energy capacity increases. Moreover, the MC battery capacity gradually increases, and the number of nodes to be charged that can complete their charging in a single cycle increases. When the MC capacity exceeds 6000 J, the effect of MC capacity on the charging service capacity of the WRSN system saturates, and the average SN waiting time of all strategies stabilizes with the increase of the MC capacity.

Fig. 7b shows that MC's average charging service distance decreases with the increase of MC capacity and eventually stabilizes. When the MC battery capacity is small, its charging service capacity is not adequate to complete the nodes' charging service demand and needs to return to the base station to replenish energy and then continue to complete the charging task. This leads to frequent energy replenishment of the MCs to and from the base station, i.e., the average MC charging service distance increases. When the MC battery capacity gradually increases, the MC charging service capacity gradually saturates, stabilizing the MC average charging service distance. The MMCCS strategy is the first to stabilize.

Fig. 7c highlights that the node energy hole rate decreases with the increase of MC capacity. Increasing the MC capacity on a single MC setup has a significantly lower impact on the charging service capacity of the WRSN system compared to a multi-MC system. Moreover, the NJNP strategy always has a higher WRSN energy hole rate than the other strategies. The HC strategy uses a fixed charging sequence list, and the charging synergy is poor in real-time, ignoring the charging requests of the nodes during the charging cycle. The node energy hole rate in MMCCS is significantly higher than the TSCCS and MMCCS strategies because MMCCS is a static partitioning and dynamic coordination scheme, effectively improving the MC charging efficiency and reducing the node energy hole rate compared to the other three strategies.

Fig. 7d shows that the network lifetime grows parabolically with the increase of MC battery capacity. the MC charging capacity of the NJNP strategy saturates with the increase of
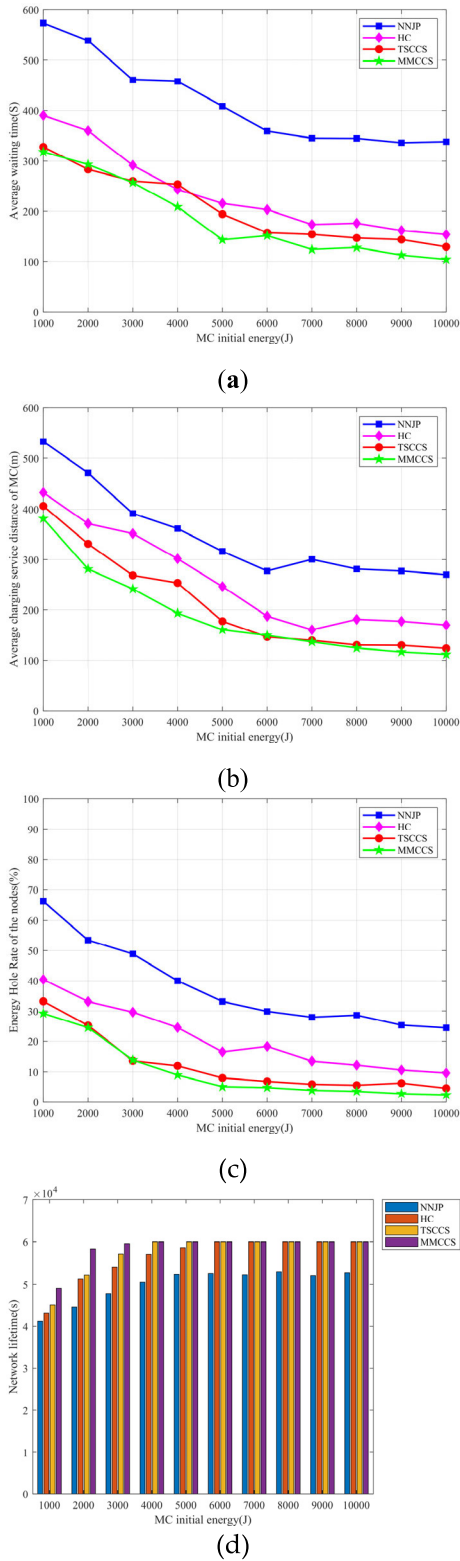
FIGURE 7. Effect of MC capacity on performance. (a) SN average waiting time; (b) MC average charging service distance; (c) WRSN energy void rate;(d) Network lifetime.

MC battery capacity, and its network survival time growth trend is relatively slow and stops stabilizing when the lifetime grows to 52500s. As the MC battery capacity increases to

5000J, the lifetime of both the TSCCS strategy and MMCCS strategy reaches 60000s, where the MMCCS strategy grows more rapidly, while the HC strategy reaches 60000s when the MC battery capacity is 5000J.

3) IMPACT OF CHARGING EFFICIENCY ON THE PERFORMANCE

This subsection investigates the effect of MC on the performance of each strategy considering SN charging efficiency. The ideal value of MC on SN charging efficiency is gradually increased from 50mJ/s to 500mJ/s with a 50mJ/s interval, and the other parameters are the default. The performance change of each strategy is illustrated in Figure 8. When the charging efficiency is between 300mJ/s-500mJ/s, the energy hole rate of WRSN is low, and WRSN maintains a healthy and good operation state, avoiding network paralysis.

Fig. 8a illustrates that the average node waiting time decreases for all strategies as the charging efficiency increases. The node average waiting time is limited by the charging time of the other nodes and the MC path movement time. Moreover, the charging time decreases due to the increased charging efficiency of MC to SN, leading to a subsequent decrease in the node average waiting time.

From Fig. 8b, the average MC charging service distance decreases slowly as the charging efficiency of MC to SN increases. When the charging efficiency is small, the number of charging services performed by MC per unit time is small, and as the charging capacity of MC increases, the number of charging service nodes performed by MC per unit time increases, and more dense nodes are served, i.e., the average charging service distance of MC decreases. The MMCCS strategy considers the network minimum energy void node as the goal for path planning and chooses a relatively far away node as the next charging node. Thus, when the MC speed is higher, the MC average charging service distance is slightly higher than the TSCCS strategy.

Fig. 8c highlights that the node energy hole rate of all strategies decreases with the increase of the charging efficiency. When the charging efficiency is low, all strategies' WRSN energy hole rates are relatively large. This is because the MMCCS strategy establishes a concentric circular charging request threshold for the WRSN network, which improves the fairness of MC response to SN charging requests and makes the energy hole rate of the MMCCS strategy consistently lower than the other three strategies. When the charging efficiency is 513mJ/s, the WRSN energy hole rate infinitely converges to zero, demonstrating the MMCCS strategy's superior performance.

Fig. 8d shows that each strategy's network lifetime increases with the charging efficiency. When the charging efficiency increases to 250mJ/s, the network lifetime of the MMCCS strategy is the first to stabilize with 60000s, while both HC and TSCCS strategies reach 60000s at a charging efficiency of 300mJ/s. When the charging efficiency increases to 500mJ/s, the lifetime of the NJNP strategy is 52630s, which stabilizes.
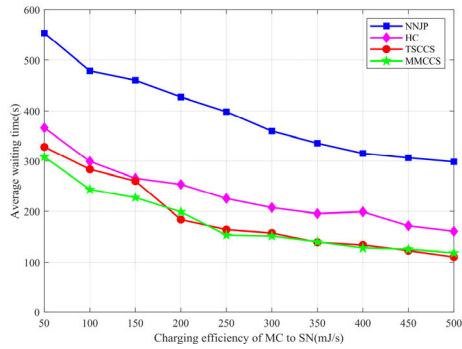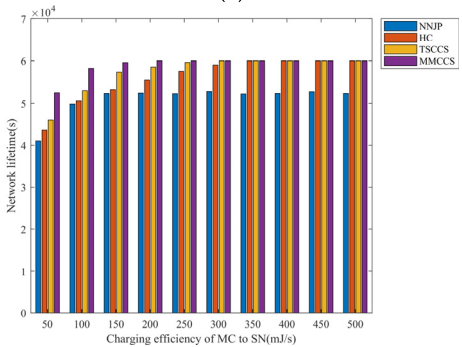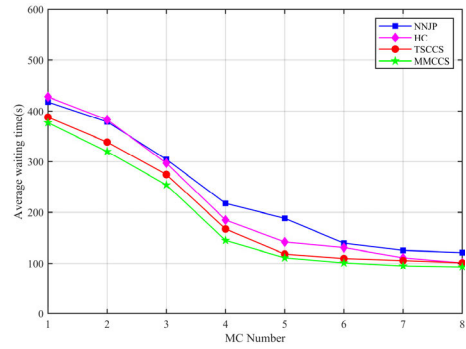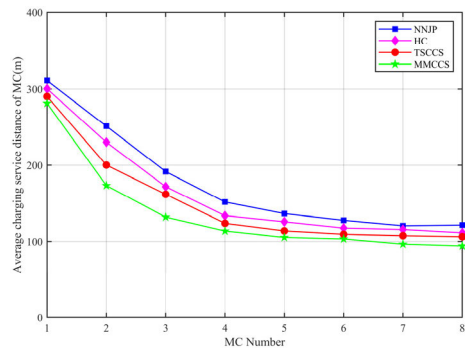
(a)
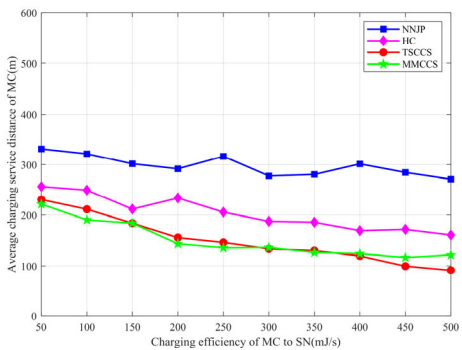
(b)
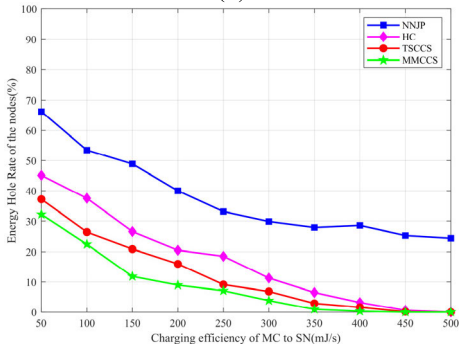
(c)

(d)

FIGURE 8. Effect of charging efficiency on the performance. (a) SN average waiting time; (b) MC average charging service distance; (c) WRSN energy void rate;(d) Network lifetime.

(a)

(b)

(c)

(d)

FIGURE 9. The impact of the number of MCs on performance. (a) SN average waiting time; (b) MC average charging service distance; (c) WRSN energy void rate;(d) Network lifetime.
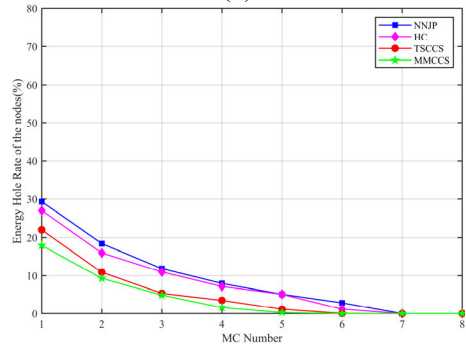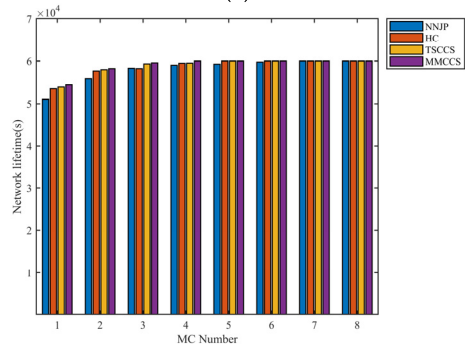
4) IMPACT OF THE NUMBER OF MC ON PERFORMANCE
This group of experiments discusses the effect of the number of MCs on the performance of each policy. In this paper,

the number of MCs is gradually increased from 1 to 8 at the interval of 1 MC, and the other parameters are kept as default values, and the performance of each policy changes

as shown in Figure 9. When the number of MCs is greater than or equal to 4, the performance of WRSN network is good. Considering the economic cost and performance of the network, the optimal number of MCs is 4.

In Figure 9a, it is shown that the average waiting time of nodes decreases for all four strategies as the number of MCs increases. the energy replenishment capacity of WRSN increases with the number of MCs, and when the number of MCs is small, the average waiting time of SN rapidly decreases with the number of MCs. when the number of MCs increases to four, the energy replenishment of the network is larger than the energy consumption of the network, and the demand of WRSN for MC saturation occurs, then the average waiting time tends to stabilize.

Figure 9b shows that with the increase of the number of MCs, the MC average charging service distance of each strategy has the same trend, and the MC average charging service distance first decreases rapidly and then stabilizes gradually. The MMCCS strategy and TSCCS strategy both adopt the zoning mode, and their MC average charging service distance is always smaller than the other two strategies.

In Figure 9c, it is shown that the node energy hole rate of all four strategies decreases with the increase of the number of MCs. When the number of MCs is 1, the WRSN energy hole rate of all four strategies is relatively large, and when the number of MCs increases to 5, the WRSN energy hole rate of the MMCCS strategy infinitely tends to 0, showing the superior performance of the MMCCS strategy.

In Figure 9d, it is shown that the network survival time of each strategy increases with the increase of the number of MCs. When the number of MCs increases to 4, the network survival time of MMCCS strategy is the first to stabilize at 60000s, while both HC and TSCCS strategies reach 60000s at a charging efficiency of 5. This reflects the better energy utilization of MMCCS strategy.

VI. CONCLUSION

This paper studies the problem of multi-MC cooperative charging in wireless rechargeable sensor networks and proposes a static partitioning plus dynamic cooperative online charging strategy MMCCS for multiple mobile charging devices aiming to reduce the energy hole rate of WRSN. The proposed strategy integrates the dynamicity and variability of sensor nodes, establishes a dual partitioning model of WRSN, and minimizes the number of energy-void nodes by online planning of multi-MC cooperative charging paths. The MMCCS strategy effectively reduces the energy hole rate of the WRSN, thus ensuring the WRSN's stable operation. Moreover, the superior performance and scalability of the MMCCS strategy affords extending it to more sensor nodes.

REFERENCES

[1] M. E. Haque and U. Baroudi, "Ambient self-powered cluster-based wireless sensor networks for industry 5.0 applications," *Soft Comput.*, vol. 25, no. 3, pp. 1859–1885, Feb. 2021, doi: 10.1007/s00500-020-05259-y.

[2] Y. Padmanaban and M. Muthukumarasamy, "Scalable grid-based data gathering algorithm for environmental monitoring wireless sensor networks," *IEEE Access*, vol. 8, pp. 79357–79367, 2020, doi: 10.1109/ACCESS.2020.2990999.

[3] S. Hegde, K. T. Min, J. Moore, P. Lundrigan, N. Patwari, S. Collingwood, A. Balch, and K. E. Kelly, "Indoor household particulate matter measurements using a network of low-cost sensors," *Aerosol Air Quality Res.*, vol. 20, no. 2, pp. 381–395, 2020, doi: 10.5209/aaqr.2019.01.0056.

[4] S. Misra, S. K. Roy, A. Roy, M. S. Obaidat, and A. Jha, "MEGAN: Multipurpose energy-efficient, adaptable, and low-cost wireless sensor node for the Internet of Things," *IEEE Syst. J.*, vol. 15, no. 1, pp. 151–155, Mar. 2020, doi: 10.1109/JSYST.2019.2920099.

[5] K. Nitesh, A. Kaswan, and P. K. Jana, "Energy density based mobile sink trajectory in wireless sensor networks," *Microsyst. Technol.*, vol. 25, no. 5, pp. 1771–1781, May 2019, doi: 10.1007/s00552-017-3569-5.

[6] G. Xu, G. Shan, and Y. Zhang, "A new energy efficient management approach for wireless sensor networks in target tracking," *Defence Technol.*, vol. 17, no. 3, pp. 932–957, Jun. 2021, doi: 10.1016/j.dt.2020.05.022.

[7] A. N. Sakib, M. Drieberg, S. Sarang, A. A. Aziz, N. T. T. Hang, and G. M. Stojanović, "Energy-aware QoS MAC protocol based on prioritized-data and multi-hop routing for wireless sensor networks," *Sensors*, vol. 22, no. 7, p. 2598, Mar. 2022, doi: 10.3390/s22072598.

[8] H. Guo, R. Wu, B. Qi, and C. Xu, "Deep-Q-networks-based adaptive dual-mode energy-efficient routing in rechargeable wireless sensor networks," *IEEE Sensors J.*, vol. 22, no. 10, pp. 9956–9966, May 2022, doi: 10.1109/JSEN.2022.3163368.

[9] A. Boudries, M. Amad, and P. Siarry, "Novel approach for replacement of a failure node in wireless sensor network," *Telecommun. Syst.*, vol. 65, no. 3, pp. 350–351, Jul. 2017, doi: 10.1007/s11235-016-0236-5.

[10] G. Ramonet and T. Noguchi, "Node replacement method for disaster resilient wireless sensor networks," in *Proc. 10th Annu. Comput. Commun. Workshop Conf. (CCWC)*. Las Vegas, NV, USA, Jan. 2020, pp. 0789–0795, doi: 10.1109/CCWC57525.2020.9031271.

[11] F. Deng, X. Yue, X. Fan, S. Guan, Y. Xu, and J. Chen, "Multisource energy harvesting system for a wireless sensor network node in the field environment," *IEEE Internet Things J.*, vol. 6, no. 1, pp. 918–927, Feb. 2019, doi: 10.1109/JIOT.2018.2865531.

[12] M. Li, Y. Xiao, and C. Xiong, "Short-term solar energy prediction method based on improved WCMA," *Yi Qi Yi Biao Xue Bao*, vol. 51, no. 10, pp. 92–99, 2020, doi: 10.19650/j.cnki.cjsi.J2006808.

[13] P. Zhou, C. Wang, and Y. Yang, "Design of self-sustainable wireless sensor networks with energy harvesting and wireless charging," *ACM Trans. Sensor Netw.*, vol. 17, no. 5, pp. 1–38, Jul. 2021, doi: 10.1155/3559081.

[14] S.-S. Tzeng and Y.-J. Lin, "Wireless energy transfer policies for cognitive radio based MAC in energy-constrained IoT networks," *Telecommun. Syst.*, vol. 77, no. 3, pp. 535–559, Jul. 2021, doi: 10.1007/s11235-021-00771-5.

[15] N. Shinohara, "Trends in wireless power transfer: WPT technology for energy harvesting, mllimeter-Wave/THz rectennas, MIMO-WPT, and advances in near-field WPT applications," *IEEE Microw.*, vol. 22, no. 1, pp. 56–59, Jan. 2021, doi: 10.1109/MMM.2020.3027935.

[16] K. Sabale and S. Mini, "Transmission power control for anchor-assisted localization in wireless sensor networks," *IEEE Sensors J.*, vol. 21, no. 8, pp. 10102–10111, Apr. 2021, doi: 10.1109/JSEN.2021.3054372.

[17] G. K. Ijemaru, K. L.-M. Ang, and J. K. Seng, "Wireless power transfer and energy harvesting in distributed sensor networks: Survey, opportunities, and challenges," *Int. J. Distrib. Sensor Netw.*, vol. 18, no. 3, Mar. 2022, Art. no. 155015772110677, doi: 10.1177/15501577211067750.

[18] Y. Feng, L. Guo, X. Fu, and N. Liu, "Efficient mobile energy replenishment scheme based on hybrid mode for wireless rechargeable sensor networks," *IEEE Sensors J.*, vol. 19, no. 21, pp. 10131–10153, Nov. 2019, doi: 10.1109/JSEN.2019.2928169.

[19] C. Hu, Y. Wang, and H. Wang, "Survey on charging programming in wireless rechargeable sensor networks," *J. Softw.*, vol. 27, no. 1, pp. 72–95, 2016, doi: 10.13328/j.cnki.jos.005883.

[20] L. He, L. Kong, Y. Gu, J. Pan, and T. Zhu, "Evaluating the on-demand mobile charging in wireless sensor networks," *IEEE Trans. Mobile Comput.*, vol. 14, no. 9, pp. 1861–1875, Sep. 2015, doi: 10.1109/TMC.2014.2368557.

[21] C. Lin, Z. Wang, D. Han, Y. Wu, C. W. Yu, and G. Wu, "TADP: Enabling temporal and distantial priority scheduling for on-demand charging architecture in wireless rechargeable sensor networks," *J. Syst. Archit.*, vol. 70, pp. 26–38, Oct. 2016, doi: 10.1016/j.sysarc.2016.05.005.

[22] C. Lin, J. Zhou, C. Guo, H. Song, G. Wu, and M. S. Obaidat, "TSCA: A temporal-spatial real-time charging scheduling algorithm for on-demand architecture in wireless rechargeable sensor networks," *IEEE Trans. Mobile Comput.*, vol. 17, no. 1, pp. 211–225, Jan. 2018, doi: 10.1109/TMC.2017.2703095.

[23] J.-Q. Zhu, Y. Feng, H.-Z. Sun, M. Liu, and Z.-N. Zhang, "Energy starvation avoidance mobile charging for wireless rechargeable sensor networks," *Ruan Jian Xue Bao*, vol. 29, no. 12, pp. 3868–3885, 2018, doi: 10.13328/j.cnki.jos.005315.

[24] C. Hu and Y. Wang, "Minimizing the number of mobile chargers to keep large-scale WRSNs working perpetually," *Int. J. Distrib. Sensor Netw.*, vol. 11, no. 6, Jun. 2015, Art. no. 782952, doi: 10.1155/2015/782952.

[25] S. Zhang and J. Wu, "Collaborative mobile charging," in *Wireless Power Transfer Algorithms, Technologies and Applications in Ad Hoc Communication Networks*, S. Nikoletseas, Y. Yang, A. Georgiadis, Eds. Cham, Switzerland: Springer, 2016, pp. 505–531, doi: 10.1007/978-3-319-56810-5_19.

[26] Z. Lyu, Z. Wei, J. Pan, H. Chen, C. Xia, J. Han, and L. Shi, "Periodic charging planning for a mobile WCE in wireless rechargeable sensor networks based on hybrid PSO and GA algorithm," *Appl. Soft Comput.*, vol. 75, pp. 388–503, Feb. 2019, doi: 10.1016/j.asoc.2018.11.022.

[27] Z. Lyu, Z. Wei, Y. Lu, X. Wang, M. Li, C. Xia, and J. Han, "Multi-node charging planning algorithm with an energy-limited WCE in WRSNs," *IEEE Access*, vol. 7, pp. 57155–57170, 2019, doi: 10.1109/ACCESS.2019.2909778.

[28] Y. Dong, S. Li, G. Bao, and C. Wang, "An efficient combined charging strategy for large-scale wireless rechargeable sensor networks," *IEEE Sensors J.*, vol. 20, no. 17, pp. 10306–10315, Sep. 2020, doi: 10.1109/JSEN.2020.2990641.

[29] R.-H. Cheng, C. W. Yu, C. Xu, and T.-K. Wu, "A distance-based scheduling algorithm with a proactive bottleneck removal mechanism for wireless rechargeable sensor networks," *IEEE Access*, vol. 8, pp. 158906–158925, 2020, doi: 10.1109/ACCESS.2020.3015911.

[30] R. Du, L. Gkatzikis, C. Fischione, M. Xiao, "On maximizing sensor network lifetime by energy balancing," *IEEE Trans. Netw. Syst.*, vol. 5, no. 3, pp. 1206–1218, Sep. 2018, doi: 10.1109/TCNS.2017.2696363.

[31] X. Lu, P. Wang, D. Niyato, D. I. Kim, and Z. Han, "Wireless charging technologies: Fundamentals, standards, and network applications," *IEEE Commun. Surveys Tuts.*, vol. 18, no. 2, pp. 1513–1552, 2nd Quart., 2016, doi: 10.1109/COMST.2015.2599783.

[32] C. Sha, Y. Sun, and R. Malekian, "Research on cost-balanced mobile energy replenishment strategy for wireless rechargeable sensor networks," *IEEE Trans. Veh. Technol.*, vol. 69, no. 3, pp. 3135–3150, Mar. 2020, doi: 10.1109/TVT.2019.2962877.

[33] G. Han, X. Yang, L. Liu, and W. Zhang, "A joint energy replenishment and data collection algorithm in wireless rechargeable sensor networks," *IEEE Internet Things J.*, vol. 5, no. 5, pp. 2596–2605, Aug. 2018, doi: 10.1109/JIOT.2017.2785578.

[34] R. Anwit, A. Tomar, and P. K. Jana, "Tour planning for multiple mobile sinks in wireless sensor networks: A shark smell optimization approach," *Appl. Soft Comput.*, vol. 97, Dec. 2020, Art. no. 106802, doi: 10.1016/j.asoc.2020.106802.

[35] H.-R. Cao, Z. Yang, X.-J. Yue, and Y.-X. Liu, "An optimization method to improve the performance of unmanned aerial vehicle wireless sensor networks," *Int. J. Distrib. Sensor Netw.*, vol. 13, no. 5, Apr. 2017, Art. no. 155015771770561, doi: 10.1177/1550157717705615.

[36] J. Yang, J.-S. Bai, and Q. Xu, "An online charging scheme for wireless rechargeable sensor networks based on a radical basis function," *Sensors*, vol. 20, no. 1, p. 205, Dec. 2019, doi: 10.3390/s20010205.

YANG JIA received the B.S. degree in testing and metrology from Xinjiang University, in 1997 and the M.S. and Ph.D. degrees in automation from Chongqing University, in 2003 and 2009, respectively. Since 2009, he has been working as an Associate Professor with the School of Electrical and Electronic Engineering, Chongqing University of Technology. His research interests include wireless sensor networks, evolutionary algorithms, and control theory.

WANG JIAHAO received the bachelor's degree in engineering from the Chongqing University of Technology, in 2020, where he is currently pursuing the master's degree in energy power. His research interests include wireless rechargeable sensor networks.
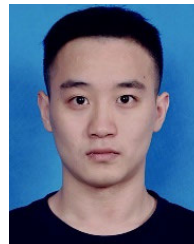
JI ZEYU received the bachelor's degree in engineering from Tianjin Urban Construction University, in 2020. He is currently pursuing the master's degree in energy power with the Chongqing University of Technology. His research interests include the positioning of mobile robot.

PENG RUIZHAO received the bachelor's degree in engineering from the Taizhou Institute of Science and Technology, in 2020. He is currently pursuing the master's degree in energy power with the Chongqing University of Technology. His research interests include sensor network routing optimization algorithm.

• • •